

# Development of the MPAS-CMAQ Coupled System (V1.0) for Multiscale Global Air Quality Modeling

David C. Wong<sup>1,\*</sup>, Jeff Willison<sup>1,\*</sup>, Jonathan E. Pleim<sup>1</sup>, Golam Sarwar<sup>1</sup>, James Beidler<sup>1</sup>, Russ Bullock<sup>1</sup>, Jerold A. Herwehe<sup>1</sup>, Rob Gilliam<sup>1</sup>, Daiwen Kang<sup>1</sup>, Christian Hogrefe<sup>1</sup>, George Pouliot<sup>1</sup>, and Hosein Foroutan<sup>2</sup>

<sup>1</sup>Office of Research and Development, U.S. Environmental Protection Agency, Durham, NC USA

<sup>2</sup>Department of Earth and Atmospheric Science, University of Houston, TX USA

<sup>3</sup>Civil & Environmental Engineering, Virginia Tech, Blacksburg, VA USA

\*These authors contributed equally to this work.

**Correspondence:** David C. Wong (wong.david-c@epa.gov) Jeff Willison (willison.jeff@epa.gov) Jon Pleim (pleim.jon@epa.gov)

## Abstract.

The Community Multiscale Air Quality (CMAQ) model has been used for regulatory purposes at the US EPA and in the research community for decades. In 2012, we released the WRF-CMAQ coupled model that enables aerosol information from CMAQ to affect meteorological processes through direct effects on shortwave radiation. Both CMAQ and WRF-CMAQ are considered limited area models. Recently, we have extended domain coverage to global scale linking the meteorological Model for Prediction Across Scales - Atmosphere (MPAS-A, hereafter referred simply to as MPAS) with CMAQ to form the MPAS-CMAQ global coupled model. To configure these three different models, i.e. CMAQ (offline), WRF-CMAQ, and MPAS-CMAQ, we have developed the Advanced Air Quality Modelling System (AAQMS) for constructing each of them effortlessly. We evaluate this newly-built MPAS-CMAQ coupled model using two global configurations: a 120 km uniform mesh and a 92-25 km variable mesh with the finer area over North America. Preliminary computational tests show good scalability and model evaluation, a three years simulation (2014 - 2016) for the uniform mesh case and a monthly simulation of January and July 2016 for the variable mesh case, on ozone and PM<sub>2.5</sub>, show reasonable performance with respect to observations. The 92-25 km configuration has a high bias in wintertime surface ozone across the United States and this bias is consistent with the 120 km result. Summertime surface ozone in the 92-25 km configuration is less biased than the 120 km case. The MPAS-CMAQ system reasonably reproduces the daily variability of daily average PM from the Air Quality System (AQS) network.

## 1 Introduction

The Community Multiscale Air Quality (CMAQ) model (Byun and Schere, 2006) was developed at the U.S. Environmental Protection Agency (EPA) starting in the mid-1990s. CMAQ is an Eulerian 3-D chemistry transport model currently being used both as a regulatory model at the EPA and a research tool by scientists around the world to study various air pollution problems on regional to hemispheric scales. In offline mode, CMAQ is driven by 3-D meteorological fields provided by upstream simulations using meteorology models, such as the Weather Research and Forecasting (WRF) model (Skamarock et al., 2008).

The Meteorology-Chemistry Interface Processor (MCIP) (Otte and Pleim, 2010) is used to provide model-ready meteorological data to the CMAQ model. The process includes unit conversions, format conversions, and vertical grid resolution-related interpolations, as well as calculating additional diagnostic variables required by CMAQ not available in the meteorology model output. In addition to the hourly meteorological data typically produced by MCIP, running CMAQ in offline mode also relies on initial and lateral boundary conditions for chemical constituents (which are created by extraction and interpolation from a larger scale chemistry-transport model), and emissions data. Drawbacks of the regional-to-hemispheric offline configuration are errors introduced by the constant temporal interpolation of meteorological data to a advection time step needed by CMAQ, as well as a lack of feedbacks between the air quality model and the meteorological model (note that CMAQ impacts WRF and in turn WRF impacts CMAQ and thus it is a two-way interaction).

These drawbacks led to linking CMAQ with WRF to form the WRF-CMAQ coupled model in 2008 (Wong et al., 2012) which included aerosol direct radiative effects. This is an online model where the meteorological information is sent to CMAQ at a user-specified frequency and the aerosol information is fed back to WRF, affecting the short-wave radiation calculation. The implementation of aerosol radiative effects in the WRF-CMAQ model and a demonstration of its impacts on simulated meteorology and subsequent air quality (Wong et al., 2012) led to interest in exploring such interactions in heavily polluted environments (Wang et al., 2014; Xing et al., 2015), and wildfire scenarios (Wong et al., 2016). The coupled online system also eliminates meteorological temporal interpolation errors that affect offline (sequential) meteorology-AQ systems. More recently, the CMAQ model and the WRF-CMAQ coupled model were extended from regional scale to hemispheric coverage (Mathur et al., 2017).

However, there are still limitations to the WRF-CMAQ coupled model, which include inconsistencies in dynamics between WRF and CMAQ, boundary condition requirements from different global chemistry models which compound into a chemical species mapping problem, and grid structure differences between global and regional models within the WRF-CMAQ coupled model. In addition, multiple grid nesting from hemispheric to local scales adds interpolation errors at every step of refinement. The National Center for Atmospheric Research (NCAR) has recently developed a new global meteorological model, the Model for Prediction Across Scales – Atmosphere (Skamarock et al., 2012) (MPAS-A, hereafter referred to as MPAS), which uses a predominantly hexagonal mesh to provide spatial refinement that minimizes discontinuities from global to regional scales. MPAS can be configured with high resolution for regions of interest with seamless transition to coarser resolution for the rest of the globe. In this study, we describe the development of a system to link MPAS with CMAQ to form a global coupled modeling system. This new modeling system will eliminate need for multiple nested modeling domains as well as spatial interpolation errors to enable more robust examinations of the impacts of international transport on modulating background concentrations that will aid multiple objectives including the national ambient air quality standards (NAAQS) and continued progress towards regional haze goals.

A brief description of the numerical model components of the MPAS-CMAQ coupled model is provided in Section 2. The depiction of the other components of the MPAS-CMAQ coupled model is given in Section 3. Section 4 presents the general performance of this new coupling system, while Section 5 summarizes the main results and lays out future work.

## 2 Overview of scientific components of the coupled model

The MPAS-CMAQ coupled model was constructed based upon the development of the Advanced Air Quality Modelling System (AAQMS) platform (Fig. 1). This platform provides a flexible environment for modelers to construct the offline CMAQ model, the WRF-CMAQ coupled model, or the MPAS-CMAQ coupled model. The meteorological and air quality model layers of the AAQMS will be described in this section, and the other two layers, unified coupler, and MIO (Model I/O), will be described in section 3.

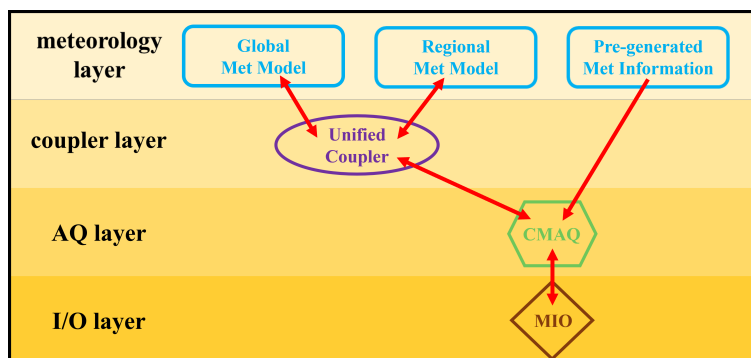


**Figure 1.** Synopsis of the Advanced Air Quality Modeling System (AAQMS). Arrows indicate the flow of information.

### 2.1 MPAS

MPAS is a global meteorological model performing computations on an unstructured mesh with primarily hexagons, as well as some pentagons and heptagons. Unstructured meshes can be uniform (Fig 2 left) or with one or more focus area(s) of seamless mesh refinement (Fig. 2 right). The dynamical equations numerically solved by the MPAS model are fully compressible, Euler nonhydrostatic, and are conservative for all scalar variables. The prognostic variables are the three velocity components, perturbation potential temperature, perturbation geopotential, and perturbation air surface pressure. Additional prognostic variables depend on the model physics options and may include turbulent kinetic energy, water vapor mixing ratio, and several cloud microphysical scalars such as cloud water and ice mixing ratio, rain and snow mixing ratio, and graupel mixing ratio. Both the MPAS and the CMAQ model are configured with the exact same grid configurations and coordinate systems. Thus, no spatial interpolation of either meteorological or chemical data is required.

MPAS source code is publicly available on github (<https://github.com/MPAS-Dev/MPAS-Model>). The MPAS portion of this coupled model is based on version 7.0 with additional modifications described in the following two sub-sections.

#### 2.1.1 MPAS model enhancements

Additional enhancements were necessary in order to use MPAS for retrospective air quality simulations. Specifically, several physics models which are associated with specific physics options in the namelist, namely the Pleim-Xiu land-surface

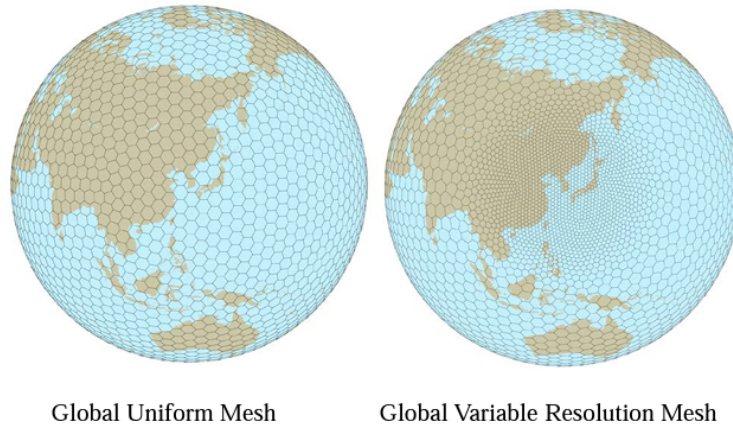


**Figure 2.** MPAS unstructured uniform mesh (left) and unstructured variable mesh with one area of refinement (right). source: <https://www.ecmwf.int/sites/default/files/elibrary/2012/14043-global-nonhydrostatic-atmospheric-model-mpas-preliminary-results-uniform-and-variable.pdf>

model (PX LSM) (Pleim and Xiu, 1995, 2003; Xiu and Pleim, 2001), the Asymmetric Convective Model 2 (ACM2) planetary boundary layer scheme (Pleim, 2007a, b), the Pleim surface layer scheme (Pleim, 2006), and the subgrid-scale convective cloud feedback to the radiation schemes (Alapaty et al., 2012) were added to MPAS. Existing MPAS physics options are generally expected to be skillful at simulating atmospheric conditions associated with extreme weather. The physics options used here were designed to improve meteorological conditions that influence atmospheric chemistry and EPA commonly uses these options for retrospective air quality modeling (e.g. Appel et al. (2021)). Gilliam et al. (2021) provides a thorough MPAS model performance evaluation with these new options. Additionally, the Four-Dimensional Data Assimilation (FDDA), using a method similar to analysis nudging in WRF but adapted to the polygonal Voronoi mesh in MPAS, was added. The FDDA method is described in (Bullock Jr. et al., 2018) along with test simulations conducted for January and July 2013 showing the new FDDA option constrains model errors relative to both the target fields used for FDDA and standard meteorological observations, while still maintaining the conservation of mass reasonably.

### 2.1.2 Transport processes

The WRF-CMAQ coupled model is designed to have two independent and different transport algorithms within WRF and CMAQ to handle the dynamic processes and chemical species, respectively. However, in the MPAS-CMAQ coupled model, the transport portion of the code within CMAQ (horizontal and vertical advection as well as horizontal diffusion) is turned off and all transport is handled by the MPAS model for consistency. At the end of the CMAQ step, all the chemical species information is transferred to MPAS as scalars. Once they have gone through the transport process and the end of the MPAS step has been reached, they are then transferred back to CMAQ and this cycle repeats itself. These new scalars are added in

95 the MPAS Registry.xml file before compilation. Since CMAQ supports multiple chemical mechanisms with different species, a simple Fortran code was created as a tool to facilitate adding new scalars into the registry file.

## 2.2 CMAQ

CMAQ (Appel et al., 2021) is a 3-D Eulerian atmospheric chemistry and transport model that numerically integrates a set of interdependent mass conservation equations for various chemical species. The CMAQ model employs operator splitting to modularize the various physical and chemical processes including subgrid turbulent vertical transport, horizontal and vertical advection, horizontal diffusion, cloud processes (i.e., aqueous chemistry, subgrid convective transport, wet deposition), gas-phase chemistry, and aerosol chemistry and dynamics. The CMAQ system also ingests anthropogenic and wildfire emission rates typically processed by the Sparse Matrix Operator Kernel Emissions (SMOKE, <http://www.cep.unc.edu/empd/products/smoke>). Plume rise, biogenic and natural emissions, and dry deposition are all modeled components of the CMAQ model. Both sources (emissions) and sinks (deposition) are applied as mass tendencies in the vertical diffusion calculation. In this study we use CMAQ v5.4, publicly available on github (<https://github.com/USEPA/CMAQ>).

## 3 Other Layers of the Coupled Model

The details of the remaining layers of the AAQMS that facilitate the construction of the MPAS-CMAQ coupled model are presented here. The unified coupler works with both the WRF-CMAQ and the MPAS-CMAQ coupled models. The I/O layer deals with I/O on the CMAQ side only.

### 3.1 Unified Coupler

The Earth System Modeling Framework (ESMF) (Hill et al., 2004) is a popular model coupler, that provides a means of exchanging data between two models. It also handles map projection conversion when the models are simulating in two different map projections, and data re-mapping/interpolation when the domain coverage and resolution are not the same in both models to ensure data exchange is done properly. There are also some couplers that are tailored for a specific application (Craig et al., 2005; Larson et al., 2005).

In this work, we adopted a simpler approach tailored for our specific application. For both the WRF-CMAQ and the MPAS-CMAQ coupled models, CMAQ inherits the domain structure from either WRF or MPAS, and therefore, the coupler inherits the map projection, grid alignment, and grid spacing seamlessly. For simplicity, we just need a straightforward mechanism for data exchange between the two models (Fig. 3).

The coupler in the WRF-CMAQ coupled model was based on the BUFFERED file (in memory) feature from IOAPI3 (Input/Output Application Programming Interface version 3, <https://www.cmascenter.org/ioapi>). CMAQ utilizes IOAPI3 to provide basic I/O functions and other supplementary functions such as time to second conversion. Due to various constraints such as character string length is 16, and lack of flexibility such as all variables are with the dimensionality, creation of this unified coupler is the first step of moving away from IOAPI3 while constructing a single universal coupler serving both the

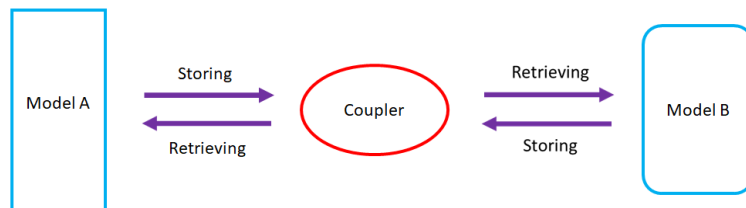


**Figure 3.** Depiction of the Unified Coupler.

WRF-CMAQ and the MPAS-CMAQ coupled models for software interoperability purposes. The data exchange occurs in both directions. Meteorological data is made available to drive the CMAQ model, and subsequently aerosol information is passed back to the meteorological model so that it can affect the radiation calculations (aerosol radiative direct effect). However, we should note that at this stage of the MPAS-CMAQ development, further work is needed to implement a robust and flexible way to represent soluble and insoluble lumped species, which are two of the five categorical components impacting the radiation calculations, with respect to different chemical mechanisms supported by CMAQ. Hence, the current MPAS-CMAQ coupled model does not yet include aerosol radiative direct effect but the coupler infrastructure will allow its implementation in future work.

The unified coupler adopted simple and straightforward strategies to handle these two major characteristic differences. For the first characteristic, in both models, 2D arrays are used. For MPAS, which arranges all mesh points linearly as a 1D array, the size of the second dimension is set to 1. For the second characteristic, we put the circular buffer dimension as the last dimension in an array with 0:1 declaration to facilitate time interpolation in the WRF-CMAQ coupled model, and defined as 1 for the MPAS-CMAQ coupled model to indicate no interpolation is necessary. With the MPAS-CMAQ coupled model, the transport is handled in MPAS and the time step in CMAQ is fully synchronized with MPAS.

### 3.1.1 MIO

All input and output files associated with MPAS, WRF, and CMAQ are in the Network Common Data Form (netCDF, <http://www.unidata.ucar.edu/packages/netcdf/index.html>) (Rew and Davis, 1990). MPAS and WRF have their own input/output (I/O) systems, while CMAQ I/O is handled by IOAPI3. The key difference is the definition and requirement of the data declaration section of the netCDF file among all these three models. The IOAPI3 I/O format has less flexibility, e.g., all variables in a given file must have the same dimensionality. Reading in emission inputs, writing calculated concentration fields, and diagnostic information are the main functions of the I/O system in CMAQ. Running the coupled model, whether it is MPAS-CMAQ or WRF-CMAQ, needs initial conditions (or the restart file), and other auxiliary input files, as well as emission files, which are critical for the chemistry transport model (CTM) CMAQ. We have examined the possibility of having the MPAS I/O system (Dennis et al., 2012) read in emission data. In this case, the MPAS I/O system would read in the emission data, the unified coupler would handle the transfer, and finally, the CMAQ model would ingest this information. For this scenario, the

MPAS registry file must be modified to include the emission species information, which is chemical mechanism dependent. In our testing, we have found this method not to be an efficient or practical pathway to reading in emission data.

To streamline I/O processes, we have developed the MIO to provide an interoperable I/O system for reading and writing in the MPAS-CMAQ, WRF-CMAQ, and CMAQ standalone models in various flavors of netCDF formats. MIO supports the traditional "pseudo" parallel output paradigm, i.e., each processor sends its own sub-domain data to the I/O processor, typically PE 0, and the I/O processor stitches the data together and writes it to the disk. MIO can also support true parallel I/O paradigm utilizing the pnetCDF library and an existing parallel file system (currently not supported for MPAS-CMAQ model). This feature has been reported in the offline CMAQ case study (Wong et al., 2015).

## 4 Coupled Model Performance

We examine the performance of this newly developed coupled system in two different ways: computational and physical aspects based on two mesh configurations (120 km uniform mesh and 92-25 km variable mesh). We did a 7-day simulation with the 120 km uniform (1/1/2016 - 1/7/2016) and a one-day (1/1/2016) test with the 92-25 km mesh to determine the computational performance. Subsequently, we did a monthly test of January and July 2016 to validate the model performance for both mesh configurations. All of the simulations were conducted on the EPA HPC system in a non-dedicated environment. On this HPC system, there are 128 compute nodes (broadwell), organized in four MPI partitions of 32 nodes each with Intel E5-2697A v4 (16 cores, 2.6 GHz) and 32 compute nodes (cascadelake) with Intel 6248R (24 cores, 3.0 GHz) in one single MPI partition. For consistency purposes, only broadwell nodes were used.

### 4.1 Model setup

Each MPAS and CMAQ model allows various combinatorial options for running the model. On the MPAS side, we followed the same set of physics options that were used in a recent study (Gilliam et al., 2021): WSM6 single-moment microphysics (Hong and Lim, 2006); Kain-Fritsch convection (Kain, 2004) modified to provide subgrid-scale cloud feedbacks to the radiation schemes (Alapaty et al., 2012; Herwehe et al., 2014) and utilizing a scale-aware dynamic convective time scale (Bullock et al., 2015); ACM2 planetary boundary layer (Pleim, 2007b); PX land surface model (Xiu and Pleim, 2001; Pleim and Xiu, 2003; Pleim and Gilliam, 2009) coupled to a PX surface layer (Pleim, 2006) with NLCD40 (CONUS) and MODIS (rest of globe) land use (Ran et al., 2016); and grid analysis nudging FDDA (Bullock Jr. et al., 2018). CMAQ is a chemical transport model and it supports different chemical mechanisms where Carbon Bond is one of them. The Carbon Bond chemical mechanism has long been used in CMAQ and we are using the CB6r5m version (Sarwar et al., 2015, 2019), which includes chlorine, bromine, and iodine chemistry to better represent the atmosphere over marine environments, in this work. CMAQ does not include a full representation of stratospheric chemistry, and the potential vorticity scaling approach that is used in hemispheric-scale CMAQ domains to estimate ozone mixing ratios in the upper layers (Xing et al., 2016) is not viable over the equator. In MPAS-CMAQ we ingest time-dependent values of stratospheric ozone from the Copernicus Atmosphere Monitoring Service (CAMS) reanalysis product (Inness et al., 2019) where model pressure is less than 300 hPa and model ozone is above 200 ppb.

We also utilized other typical settings (Appel et al., 2021) on the CMAQ side. Table 1 lists the key options which were used in this MPAS-CMAQ coupled model.

**Table 1.** Different options were used in the MPAS-CMAQ model.

MPAS	CMAQ
microphysics scheme: WSM6	chemical mechanism: CB6r5m
convection scheme: enhanced Kain-Fritsch	aerosol module: AER07
land surface model scheme: Pleim-Xiu (PX)	deposition model: M3DRY
boundary layer scheme: ACM2	chemistry solver: Rosenbrock
surface layer scheme: Pleim	
land use: NLCD40 and MODIS	

185 In general, CMAQ simulations take a much longer time than a meteorological model. One of the reasons is the stiffness of the system of ordinary differential equations involved in the chemistry step and a large number of prognostic equations for several chemical species. The MPAS-CMAQ coupled model provides a feature to allow users to choose the frequency of the data transfer between the MPAS and CMAQ models at run time. Users can balance model performance and model run time. In this study, we chose a frequency of 3:1 for the variable resolution mesh, i.e., CMAQ will be called after every three MPAS  
190 time-steps. For the uniform mesh we use a coupling frequency of 1:1. Varying this frequency does not result in systematic changes to the performance metrics presented here, but should be investigated more thoroughly in a future study.

The MPAS-CMAQ modeling requires emissions characterized on a global domain. Previous development of emissions for the hemispheric CMAQ utilized the global HTAP (Hemispheric Transport of Air Pollution, version 2) inventory (Janssens-Maenhout et al., 2015) at a  $0.1^\circ \times 0.1^\circ$  grid resolution to provide anthropogenic emissions estimates outside of North America  
195 (Eyth et al., 2016). The HTAP inventories served as the basis for global anthropogenic emissions estimates outside of North America for MPAS-CMAQ. HTAP emissions were projected from 2010 to the model scenario year using scaling factors derived from the Community Emissions Data Systems historical emissions dataset (Hoesly et al., 2018). The SMOKE modeling environment was used to temporalize the HTAP emissions to hourly rates and speciate volatile organic compounds (VOC), particulates (PM), and nitrogen oxides ( $\text{NO}_x$ ). To prepare the gridded emissions for the MPAS mesh a spatial intersection  
200 was performed between the HTAP grid and MPAS mesh. Spatial allocation factors were calculated as the area of intersection between the grid and mesh cells divided by the total area of the HTAP grid cell. The spatial allocation factors were then applied to the HTAP emissions to calculate the total emissions rate at each MPAS cell. HTAP sectors related to aviation, biomass burning, energy generation, industrial processes, and waterborne navigation were vertically allocated to 44 layers using sector-specific layer fractions. Recent inputs for MPAS-CMAQ replaced the HTAP emissions over China with emissions estimates  
205 from Tsinghua University (Zhao et al., 2018) provided on a  $27 \text{ km} \times 27 \text{ km}$  grid. The processes to temporalize, speciate, and spatially allocate the China emissions to the MPAS mesh were similar to the steps described for HTAP with replacement MPAS mesh allocation factors from the intersection of the China grid and the MPAS mesh. MPAS-CMAQ runs utilized inline MEGAN biogenic emissions rather than emissions generated in GEOS-Chem. The Fire Inventory from NCAR (FINN) v1.5

was used for wildland fire and agricultural burning emissions outside of the United States (Wiedinmyer et al., 2011). The FINN  
210 fire emissions inventories were processed through SMOKE to produce 2-D gridded emissions on the HTAP  $0.1^\circ \times 0.1^\circ$  grid.  
The gridded fire emissions were spatially and vertically allocated on the MPAS mesh using the area fractions derived for the  
HTAP grid and the biomass burning layer factors, respectively. Nitrogen oxide ( $\text{NO}_x$ ) emissions from lightning strikes and their  
vertical allocation were estimated from a set of global monthly inventories (Price et al., 1997). These lightning  $\text{NO}_x$  emissions  
were apportioned to the  $0.1^\circ \times 0.1^\circ$  HTAP grid and mapped to the MPAS mesh using the spatial factors. Lightning  $\text{NO}_x$   
215 emissions were temporalized using seasonal lightning flash rates by continent and hour (Blakeslee et al., 2014). Speciation of  
the lightning  $\text{NO}_x$  used a 90/10 split to NO and  $\text{NO}_2$ . For all global sources the emissions were converted to a flux by dividing  
the rate by the area of the mesh cell.

Emissions over North America initially relied on the 2016 EPA Emissions Modeling Platform (EPA, 2021). Subsequent  
North America emissions were developed from EPA's Air QUALity Time Series Project (EQUATES) inventories and ancillary  
220 files (Foley et al., 2023). Speciation and temporal allocation methods were performed consistent with the emissions prepared  
for the regional modeling in the 2016 modeling platform and EQUATES. Spatial surrogates were generated using modeling  
platform weighting data and a shapefile of the target MPAS mesh. Area source sector emissions were spatially allocated in  
SMOKE to the mesh using the spatial surrogates. The SMOKE output gridded emissions were merged together across sectors  
to produce a single area file with each row representing a mesh cell. A cross-reference of the area rows to the mesh cells was  
225 used to allocate emissions onto the MPAS mesh. As with the global emissions, the US and North American emissions were  
converted from a rate to a flux by dividing the emissions rate by the mesh cell area. Point emissions sources were processed  
through SMOKE for inline use in CMAQ without any additional post-processing.

## 4.2 Computational performance

We quantify the computational performance of the MPAS-CMAQ coupled system by measuring wall-clock time. For the 120  
230 km uniform mesh, there are only 40962 mesh points, so we capture the wall-clock time for one-week simulations with MPAS  
alone and the MPAS-CMAQ coupled model (Fig. 4 left panel). For the 92-25 km variable mesh case, there are 163842 mesh  
points, which is about four times number of mesh points in the 120 km uniform case, so we did a one-day test instead for  
convenience (Fig. 4 right panel).

Overall, our results demonstrate the computational efficiency with a reasonable speedup as additional cores are being uti-  
235 lized. For the 120 km uniform mesh case, the strongest benefit of parallelization occurs when increasing from 64 cores to  
128 cores for the coupled system. We observe smaller speed increases from larger numbers of cores when using stand-alone  
MPAS. The maximum number of cores tested here is 320 since efficiency is rapidly lost at this level of domain decomposition.  
For 320 cores, the MPAS simulation takes 43.3 minutes to complete and the MPAQ-CMAQ simulation takes 114.5 minutes to  
complete. For the 92-25 km variable mesh case, stand-alone MPAS performance reached a plateau with 256 cores and slightly  
240 increased the execution time with 512 cores. On the other hand, MPAS-CMAQ still performed with reasonable scalability even  
with 512 cores.

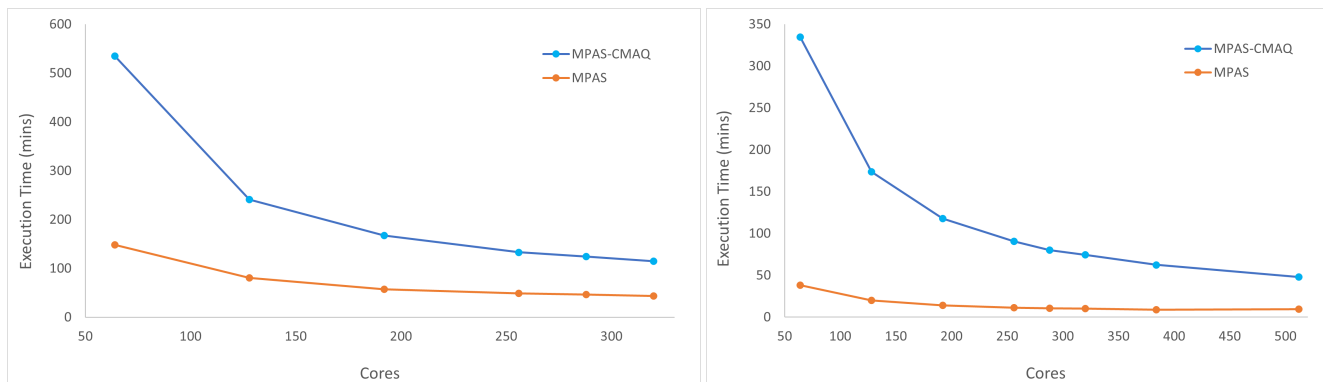


**Figure 4.** Computational performance of the MPAS (orange) and MPAS-CMAQ coupled model (blue) with 120 km uniform mesh (left) and 92-25 km variable mesh (right).

### 4.3 Preliminary Model Evaluation

The scope of this paper excludes a diagnostic accounting of the chemical processes in MPAS-CMAQ. Here we present preliminary evaluation of the system’s performance for surface air quality. We evaluate the MPAS-CMAQ system using two global configurations: a 120 km uniform mesh and a 92-25 km variable mesh with the finer area over North America. The 120 km uniform mesh allows for chemical spin up of the model at reduced computational cost. We run the 120 km configuration for a three-year period (2014-2016). The initial chemical state for the 120 km configuration is from a clean maritime profile that we apply to every cell. Initial ozone concentrations are from the CAMS reanalysis product (Inness et al., 2019) for January 1, 2014.

Modeled surface ozone follows the average interannual variability at all available Tropospheric Ozone Assessment Report, Phase II (TOAR2) sites (Fig. 5a). The time series show a consistent average wintertime high bias of about 10 ppb and a similar average low bias during spring and summer. Figure 5b shows that the high surface ozone bias in winter is consistent across the Northern Hemisphere, while Fig. 5c shows that the summertime performance is characterized by large negative biases over Europe. We observe no drift in either the magnitude of the ozone or the bias during the three year simulation. The time tendencies in both measurements and model are strikingly similar. Comparisons with ozonesondes indicate a low bias in free tropospheric ozone that peaks in springtime but the bias does not increase from 2014 to 2016 (not shown). These results give confidence in the stability of the global ozone budget in our modeling system.

The 120 km uniform mesh configuration of MPAS-CMAQ simulates summertime surface ozone that compares well with other contemporary global chemistry transport models and reanalysis products. Figure 6 shows average July surface ozone for GEOS-CF (Keller et al., 2021), MPAS-CMAQ, CAMS Reanalysis, and MERRA-2 (Gelaro et al., 2017) reanalysis. MPAS-CMAQ generally simulates lower surface ozone concentrations than the CAMS and MERRA-2 reanalysis products, but higher surface ozone than the GEOS-CF model.

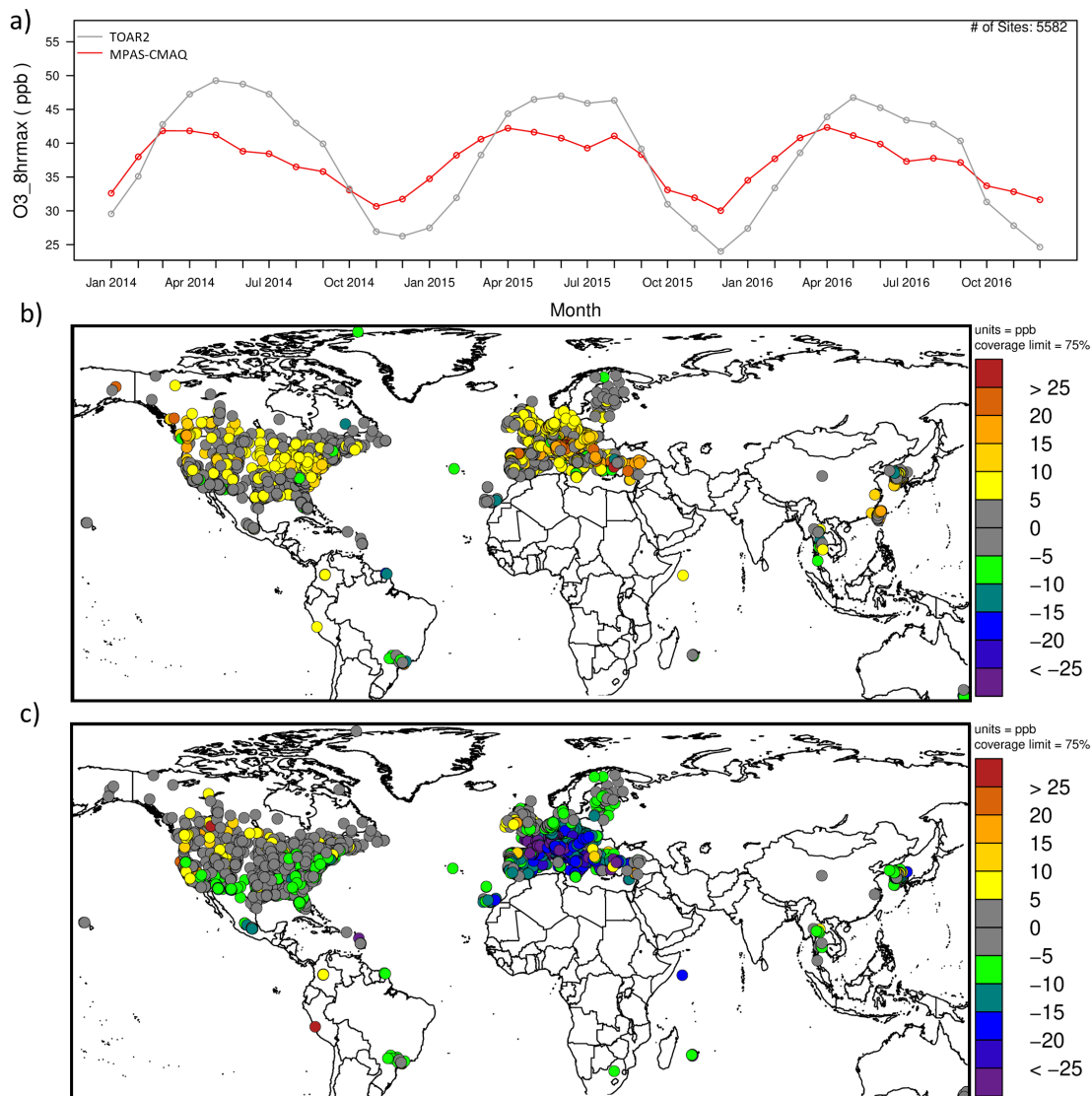


**Figure 5.** Modeled and observed surface 8-hour maximum ozone values for a) monthly average of all TOAR2 sites over time and b) average bias at each site for winter (December through February) and c) average bias at each site for summer (June through August) during the three year period.

The need for variable resolution within a consistent system motivates development of the MPAS-CMAQ framework. We test the 92-25 km variable resolution mesh with month-long simulations that we initialize from the chemical state of 120 km spin-up runs. We simulate January 2016 and July 2016 to evaluate wintertime and summertime performance. Our area of interest for these tests is the contiguous United States (CONUS) region with the refined resolution. Figure 7a shows that the 92-25 km configuration of MPAS-CMAQ also has a high bias in wintertime surface ozone across the United States. This bias

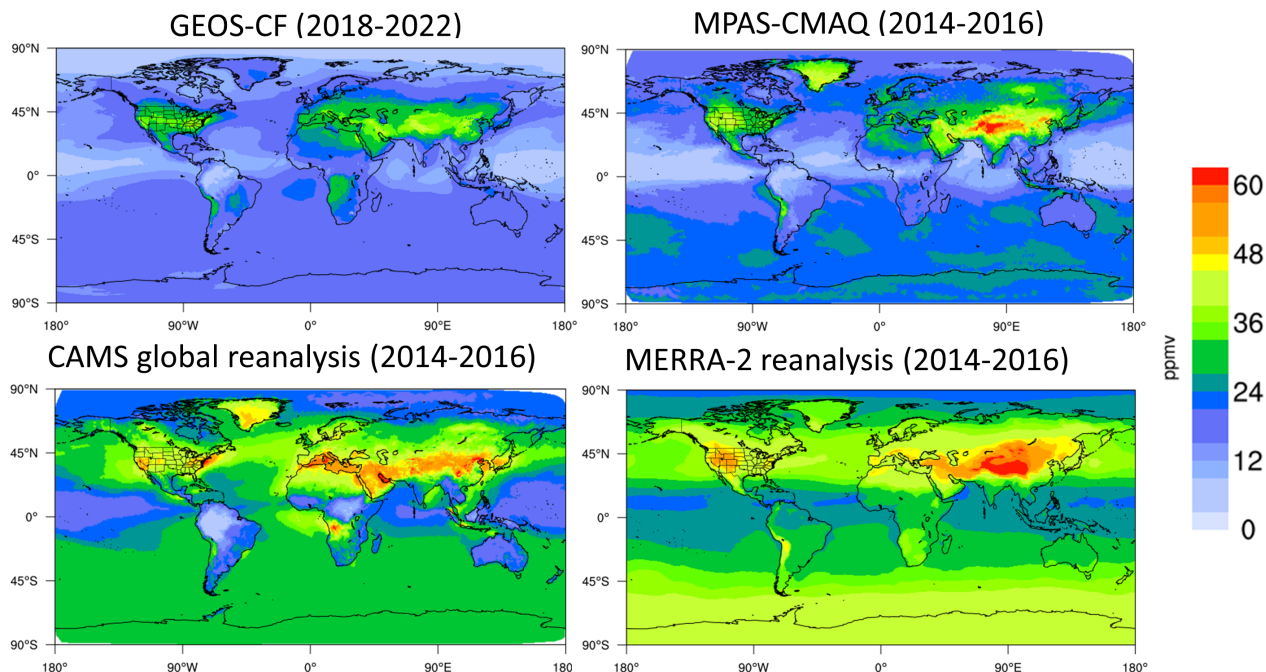


**Figure 6.** July average ozone for a) GEOS-CF, b) MPAS-CMAQ, c) CAMS reanalysis and d) MERRA-2 reanalysis.

is consistent with the 120 km result (Fig. 5a) and the EQUATES dataset. We hypothesize that emission estimates and CMAQ model chemistry drive this bias rather than meteorological sensitivities that are unique to MPAS. Summertime surface ozone  
 270 in the 92-25 km configuration is less biased as compared to uniform mesh simulations except for the well-known California central valley underestimate (Appel et al., 2021) (Fig. 7b). Again, we observe this bias in other CMAQ configurations and do not believe that it results from anything inherent to MPAS. The MPAS-CMAQ system reproduces the daily variability of daily 8-hr max ozone reasonably well (Fig. 7c, d), with mean biases of 2.8 ppb and -0.8 ppb for January and July, respectively. These CONUS-average ozone biases are similar to previous evaluations of CMAQ, including versions 5.2.1 and 5.3.1 that had  
 275 maximum absolute biases of 4-6 ppb depending on the season and configuration options (Appel et al., 2021). The photolysis of particulate nitrate may improve model ozone underestimation in California and also the general springtime ozone underestimation in the U.S. (Sarwar et al., 2024). We plan to include this chemistry in a future study as this study did not include it.

The MPAS-CMAQ system must demonstrate skill in simulating  $PM_{2.5}$  as well as ozone. The 92-25 km configuration pro-  
 280 duces a negative wintertime  $PM_{2.5}$  bias in the western US and a general high bias east of the Rocky Mountains (Fig. 8a). Emissions estimates of residential wood combustion (RWC) were unavailable for this month and are excluded for the simulation. We expect that including these emissions would increase the PM over the CONUS. The 120 km uniform simulation that includes RWC performs similarly for  $PM_{2.5}$  in January (not shown). In summertime, the bias is more consistently negative across the United States, with sporadic high biases dominating the average in the second half of the month (Fig. 8b). As with

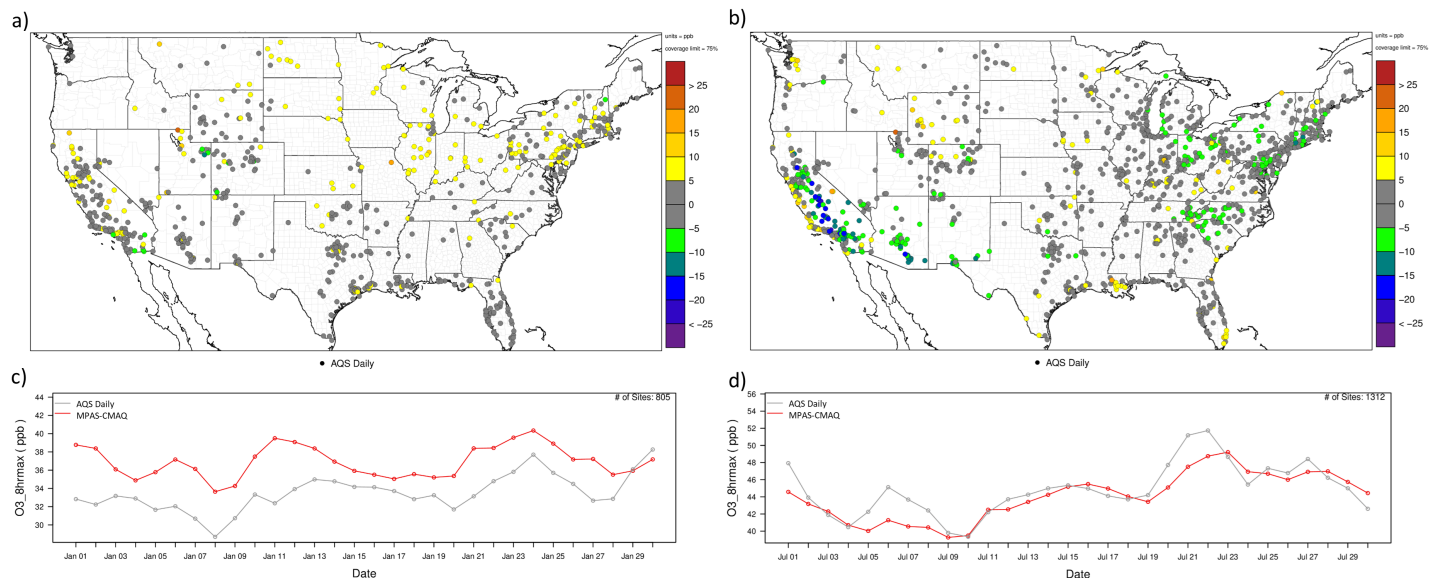


**Figure 7.** Average 8-hr max ozone bias at AQS sites for a) January 2016 and b) July 2016 on the 92-25 km variable resolution mesh. Corresponding average 8-hr max ozone mixing ratio for all AQS sites in c) January 2016 and d) July 2016.

285 ozone, the MPAS-CMAQ system reasonably reproduces the daily variability of daily average PM from the AQS network (Fig. 8c, d), with mean biases of  $-0.9 \mu\text{g}/\text{m}^3$  and  $0.1 \mu\text{g}/\text{m}^3$  for January and July, respectively. The bias for our simulations compare well with Appel et al. (2021), who reported CONUS-average biases between  $0.5\text{-}1.5 \mu\text{g}/\text{m}^3$  for CMAQ versions 5.2.1 and 5.3.1 in the months of January and July.

## 5 Conclusion and Future Work

290 We have articulately demonstrated the construction of the MPAS-CMAQ modeling system and evaluated it for the ozone simulations. Since WRF-CMAQ modeling system was already evaluated and documented in the literature, this work only focused on the evaluation of MPAS-CMAQ modeling system. The newly developed AAQMS platform which includes the unified coupler, works for all types of CMAQ configurations. This MPAS-CMAQ coupled model has theoretical advantages over the WRF-CMAQ coupled model, including consistent transport algorithms, refinement without boundary interpolation and  
 295 global coverage without polar filters. It remains to be shown whether these numerical advantages will translate to improved statistical performance metrics for simulations of retrospective air quality.

The preliminary results show the MPAS-CMAQ coupled model performed reasonably well with respect to ozone and  $\text{PM}_{2.5}$  for North America, where the fine mesh is located, as well as the rest of the world. For future work, we will implement the aerosol radiative direct effect in this coupled model with a robust and flexible method to handle different CMAQ chemical  
 300 mechanisms. We will also implement a switch so the aerosol radiative direct effect can be turned on or off at run time.

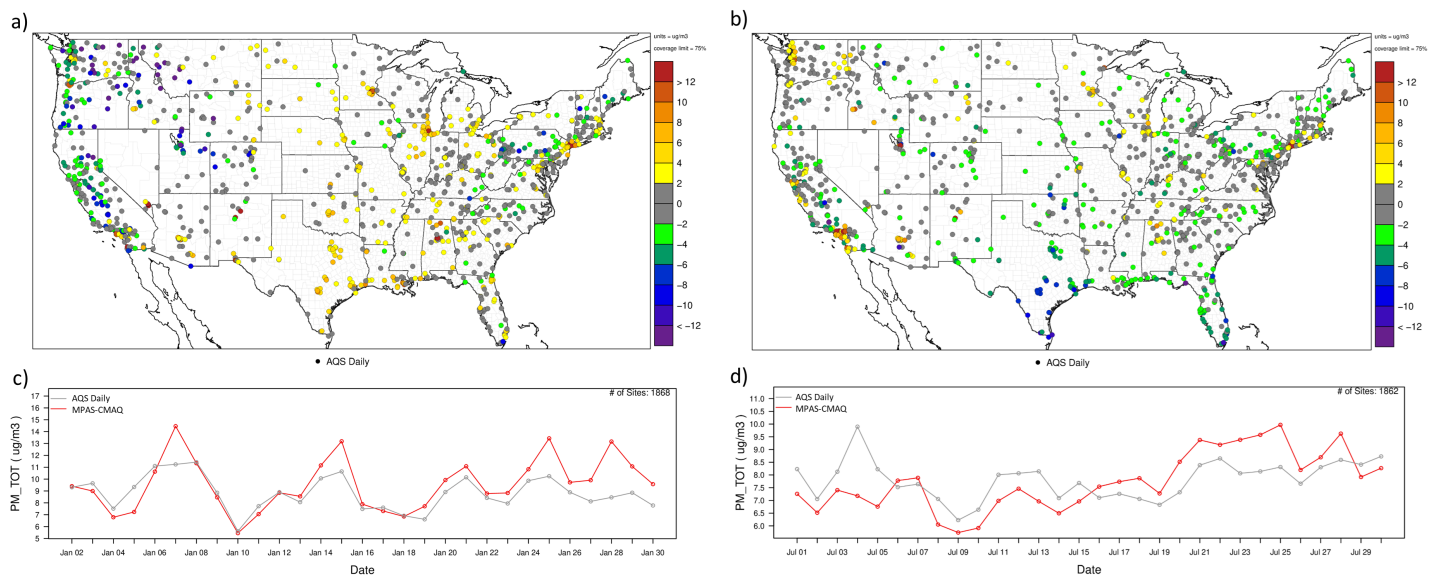


**Figure 8.** Average daily  $\text{PM}_{2.5}$  bias at AQS sites for a) January 2016 and b) July 2016 on the 92-25 km variable resolution mesh. Corresponding average daily  $\text{PM}_{2.5}$  concentration for all AQS sites in c) January 2016 and d) July 2016.

### Code and data availability

- Entire MPAS-CMAQ with internal version CMAQ 5.4 is available at Zenodo (<https://zenodo.org/records/10982421>).
- MIO is available at Zenodo (<https://zenodo.org/records/10994279>).
- data which was used in generating Figure 4 - 9, is available at Zenodo (<https://zenodo.org/records/10994244>).

305 **Author contributions** DCW defined the scope of the manuscript, developed the unified coupler, MIO, constructed the MPAS-CMAQ model. DCW, JW and JEP designed all the simulations, JW developed the MEGAN biogenic emission module and performed model evaluation. GP and JB processed emission. RB provided the FDDA updates. JH provided the EPA physics code. GS provided the marine chemistry CMAQ update. HF conducted initial scalar testing on MPAS. RG provided MPAS setup options. DK provided CMAQ lightning code update. DCW drafted the manuscript. JW, JEP, GP, RB, JH, CH, GS, HF, 310 265 RG, JB, and DK reviewed and edited the manuscript.

**Competing interests** The authors declare that they have no conflict of interest.

**Disclaimer** This paper has been subjected to an EPA review and approved for publication. The views expressed here are those of the authors and do not necessarily reflect the views and policies of the US Environmental Protection Agency (EPA).

## References

- 315 Alapaty, K., Herwehe, J. A., Otte, T. L., Nolte, C. G., Bullock, O. R., Mallard, M. S., Kain, J. S., and Dudhia, J.: Introducing subgrid-scale cloud feedbacks to radiation for regional meteorological and climate modeling, *Geophysical Research Letters*, 39, <https://doi.org/https://doi.org/10.1029/2012GL054031>, 2012.
- Appel, K. W., Bash, J. O., Fahey, K. M., Foley, K. M., Gilliam, R. C., Hogrefe, C., Hutzell, W. T., Kang, D., Mathur, R., Murphy, B. N., Napelenok, S. L., Nolte, C. G., Pleim, J. E., Pouliot, G. A., Pye, H. O. T., Ran, L., Roselle, S. J., Sarwar, G., Schwede, D. B., Sidi,  
320 F. I., Spero, T. L., and Wong, D. C.: The Community Multiscale Air Quality (CMAQ) model versions 5.3 and 5.3.1: system updates and evaluation, *Geoscientific Model Development*, 14, 2867–2897, <https://doi.org/10.5194/gmd-14-2867-2021>, 2021.
- Blakeslee, R. J., Mach, D. M., Bateman, M. G., and Bailey, J. C.: Seasonal variations in the lightning diurnal cycle and implications for the global electric circuit, *Atmospheric Research*, 135-136, 228–243, <https://doi.org/https://doi.org/10.1016/j.atmosres.2012.09.023>, 2014.
- Bullock, O. R., Alapaty, K., Herwehe, J. A., and Kain, J. S.: A Dynamically Computed Convective Time Scale for the Kain-Fritsch Convective  
325 Parameterization Scheme, *Monthly Weather Review*, 143, 2105 – 2120, <https://doi.org/10.1175/MWR-D-14-00251.1>, 2015.
- Bullock Jr., O. R., Foroutan, H., Gilliam, R. C., and Herwehe, J. A.: Adding four-dimensional data assimilation by analysis nudging to the Model for Prediction Across Scales – Atmosphere (version 4.0), *Geoscientific Model Development*, 11, 2897–2922, <https://doi.org/10.5194/gmd-11-2897-2018>, 2018.
- Byun, D. W. and Schere, K. L.: Review of the governing equations, computational algorithms, and other components of the Models-3  
330 Community Multiscale Air Quality (CMAQ) Modeling System, *Appl. Mech. Rev.*, 59, 51–77, 2006.
- Craig, A., Jacob, R., Kauffman, B., Bettge, T., Larson, J., Ong, E., Ding, C., and He, Y.: CPL6: The New Extensible, High Performance Parallel Coupler for the Community Climate System Model, *IJHPCA*, 19, 309–327, <https://doi.org/10.1177/1094342005056117>, 2005.
- Dennis, J. M., Edwards, J., Loy, R., Jacob, R., Mirin, A. A., Craig, A. P., and Vertenstein, M.: An application-level parallel I/O library for Earth system models, *The International Journal of High Performance Computing Applications*, 26, 43–53,  
335 <https://doi.org/10.1177/1094342011428143>, 2012.
- EPA: Preparation of Emissions Inventories for the 2016v1 North American Emissions Modeling Platform, Technical Support Document, [https://doi.org/https://www.epa.gov/sites/default/files/2020-11/documents/2016v1\\_emismod\\_tsd\\_508.pdf](https://doi.org/https://www.epa.gov/sites/default/files/2020-11/documents/2016v1_emismod_tsd_508.pdf), 2021.
- Eyth, A., Pouliot, G., Vukovich, J., Strum, M., Dolwick, P., Allen, C., Beidler, J., and Baek, B. H.: Development of 2011 hemispheric emissions for CMAQ, 2016 CMAS Conference,  
340 [https://doi.org/https://www.cmascenter.org/conference//2016/slides/eyth\\_development\\_hemispheric\\_2016.pptx](https://doi.org/https://www.cmascenter.org/conference//2016/slides/eyth_development_hemispheric_2016.pptx), 2016.
- Foley, K. M., Pouliot, G. A., Eyth, A., Aldridge, M. F., Allen, C., Appel, K. W., Bash, J. O., Beardsley, M., Beidler, J., Choi, D., Farkas, C., Gilliam, R. C., Godfrey, J., Henderson, B. H., Hogrefe, C., Koplitz, S. N., Mason, R., Mathur, R., Misemis, C., Possiel, N., Pye, H. O., Reynolds, L., Roark, M., Roberts, S., Schwede, D. B., Seltzer, K. M., Sonntag, D., Talgo, K., Toro, C., Vukovich, J., Xing, J., and Adams, E.: 2002-2017 anthropogenic emissions data for air quality modeling over the United States, *Data in Brief*, 47, 109022,  
345 <https://doi.org/https://doi.org/10.1016/j.dib.2023.109022>, 2023.
- Gelaro, R., McCarty, W., Suárez, M. J., Todling, R., Molod, A., Takacs, L., Randles, C. A., Darmenov, A., Bosilovich, M. G., Reichle, R., et al.: The modern-era retrospective analysis for research and applications, version 2 (MERRA-2), *Journal of climate*, 30, 5419–5454, 2017.

- Gilliam, R. C., Herwehe, J. A., Bullock Jr, O. R., Pleim, J. E., Ran, L., Campbell, P. C., and Foroutan, H.: Establishing the Suitability of the  
350 Model for Prediction Across Scales for Global Retrospective Air Quality Modeling, *Journal of Geophysical Research: Atmospheres*, 126,  
e2020JD033 588, <https://doi.org/https://doi.org/10.1029/2020JD033588>, 2021.
- Herwehe, J. A., Alapaty, K., Spero, T. L., and Nolte, C. G.: Increasing the credibility of regional climate simulations  
by introducing subgrid-scale cloud-radiation interactions, *Journal of Geophysical Research: Atmospheres*, 119, 5317–5330,  
<https://doi.org/https://doi.org/10.1002/2014JD021504>, 2014.
- 355 Hill, C., Deluca, C., Balaji, V., Suarez, M., and Da Silva, A.: Architecture of the Earth System Modeling Framework, *Computing in Science  
& Engineering*, 6, 18 – 28, <https://doi.org/10.1109/MCISE.2004.1255817>, 2004.
- Hoesly, R. M., Smith, S. J., Feng, L., Klimont, Z., Janssens-Maenhout, G., Pitkanen, T., Seibert, J. J., Vu, L., Andres, R. J., Bolt, R. M., Bond,  
T. C., Dawidowski, L., Kholod, N., Kurokawa, J.-I., Li, M., Liu, L., Lu, Z., Moura, M. C. P., O'Rourke, P. R., and Zhang, Q.: Historical  
(1750–2014) anthropogenic emissions of reactive gases and aerosols from the Community Emissions Data System (CEDS), *Geoscientific*  
360 *Model Development*, 11, 369–408, <https://doi.org/10.5194/gmd-11-369-2018>, 2018.
- Hong, S. and Lim, J.-O. J.: The WRF Single-Moment 6-Class Microphysics Scheme (WSM6), *Asia-pacific Journal of Atmospheric Sciences*,  
42, 129–151, <https://api.semanticscholar.org/CorpusID:120362377>, 2006.
- Inness, A., Ades, M., Agustí-Panareda, A., Barré, J., Benedictow, A., Blechschmidt, A.-M., Dominguez, J. J., Engelen, R., Eskes, H., Flem-  
ming, J., Huijnen, V., Jones, L., Kipling, Z., Massart, S., Parrington, M., Peuch, V.-H., Razinger, M., Remy, S., Schulz, M., and Suttie, M.:  
365 The CAMS reanalysis of atmospheric composition, *Atmospheric Chemistry and Physics*, 19, 3515–3556, <https://doi.org/10.5194/acp-19-3515-2019>, 2019.
- Janssens-Maenhout, G., Crippa, M., Guizzardi, D., Dentener, F., Muntean, M., Pouliot, G., Keating, T., Zhang, Q., Kurokawa, J., Wankmüller,  
R., Denier van der Gon, H., Kuenen, J. J. P., Klimont, Z., Frost, G., Darras, S., Koffi, B., and Li, M.: HTAP\_v2.2: a mosaic of regional  
and global emission grid maps for 2008 and 2010 to study hemispheric transport of air pollution, *Atmospheric Chemistry and Physics*, 15,  
370 11 411–11 432, <https://doi.org/10.5194/acp-15-11411-2015>, 2015.
- Kain, J. S.: The Kain-Fritsch Convective Parameterization: An Update, *Journal of Applied Meteorology*, 43, [https://journals.ametsoc.org/  
view/journals/apme/43/1/1520-0450\\_2004\\_043\\_0170\\_tkcpau\\_2.0.co\\_2.xml](https://journals.ametsoc.org/view/journals/apme/43/1/1520-0450_2004_043_0170_tkcpau_2.0.co_2.xml), 2004.
- Keller, C. A., Knowland, K. E., Duncan, B. N., Liu, J., Anderson, D. C., Das, S., Lucchesi, R. A., Lundgren, E. W., Nicely, J. M.,  
Nielsen, E., Ott, L. E., Saunders, E., Strode, S. A., Wales, P. A., Jacob, D. J., and Pawson, S.: Description of the NASA GEOS  
375 Composition Forecast Modeling System GEOS-CF v1.0, *Journal of Advances in Modeling Earth Systems*, 13, e2020MS002413,  
<https://doi.org/https://doi.org/10.1029/2020MS002413>, 2021.
- Larson, J., Jacob, R., and Ong, E.: The Model Coupling Toolkit: A New Fortran90 Toolkit for Building Multiphysics Parallel Coupled Models,  
*The International Journal of High Performance Computing Applications*, 19, 277–292, <https://doi.org/10.1177/1094342005056115>, 2005.
- Mathur, R., Xing, J., Gilliam, R., Sarwar, G., Hogrefe, C., Pleim, J., Pouliot, G., Roselle, S., Spero, T. L., Wong, D. C., , and Young, J.:  
380 Extending the Community Multiscale Air Quality (CMAQ) Modeling System to Hemispheric Scales: Overview of Process Considerations  
and Initial Applications, *Atmos Chem Phys.*, 17, 12 449–12 474, 2017.
- Otte, T. L. and Pleim, J. E.: The Meteorology-Chemistry Interface Processor (MCIP) for the CMAQ modeling system: updates through  
MCIPv3.4.1, *Geosci. Model Dev.*, 3, 243–256, 2010.
- Pleim, J. E.: A simple, efficient solution of flux-profile relationships in the atmospheric surface layer, *J. Appl. Meteor. Climatol.*, 45, 341–347,  
385 <https://doi.org/https://doi.org/10.1175/JAM2339.1>, 2006.

- Pleim, J. E.: A Combined local and nonlocal closure model for the atmospheric boundary layer. Part I: Model description and testing., *J. Appl. Meteor. Climatol.*, 46, 1383–1395, <https://doi.org/https://doi.org/10.1175/JAM2539.1>, 2007a.
- Pleim, J. E.: A Combined Local and Nonlocal Closure Model for the Atmospheric Boundary Layer. Part II: Application and Evaluation in a Mesoscale Meteorological Model, *Journal of Applied Meteorology and Climatology*, 46, 1396 – 1409, <https://doi.org/10.1175/JAM2534.1>, 2007b.
- 390 Pleim, J. E. and Gilliam, R.: An indirect data assimilation scheme for deep soil temperature in the Pleim-Xiu land surface model, *J. Appl. Meteor. Climatol.*, 48, 1362–1376, <https://doi.org/https://doi.org/10.1175/2009JAMC2053.1>, 2009.
- Pleim, J. E. and Xiu, A.: Development and Testing of a Surface Flux and Planetary Boundary Layer Model for Application in Mesoscale Models, *Journal of Applied Meteorology and Climatology*, 34, 16 – 32, [https://journals.ametsoc.org/view/journals/apme/34/1/1520-0450-34\\_1\\_16.xml](https://journals.ametsoc.org/view/journals/apme/34/1/1520-0450-34_1_16.xml), 1995.
- 395 Pleim, J. E. and Xiu, A.: Development of a land surface model. Part II: Data assimilation, *J. Appl. Meteor.*, 42, 1811–1822, 2003.
- Price, C., Penner, J., and Prather, M.: NO<sub>x</sub> from lightning: 1. Global distribution based on lightning physics, *Journal of Geophysical Research: Atmospheres*, 102, 5929–5941, <https://doi.org/https://doi.org/10.1029/96JD03504>, 1997.
- Ran, L., Pleim, J., Gilliam, R., Binkowski, F. S., Hogrefe, C., and Band, L.: Improved meteorology from an updated WRF/CMAQ modeling system with MODIS vegetation and albedo, *Journal of Geophysical Research: Atmospheres*, 121, 2393–2415, <https://doi.org/https://doi.org/10.1002/2015JD024406>, 2016.
- 400 Rew, R. K. and Davis, G. P.: NetCDF: An Interface for Scientific Data Access, *IEEE Computer Graphics and Applications*, 10, 76–82, 1990.
- Sarwar, G., Gantt, B., Schwede, D., Foley, K., Mathur, R., and Saiz-Lopez, A.: Impact of Enhanced Ozone Deposition and Halogen Chemistry on Tropospheric Ozone over the Northern Hemisphere, *Environmental Science & Technology*, 49, 9203–9211, <https://doi.org/10.1021/acs.est.5b01657>, PMID: 26151227, 2015.
- 405 Sarwar, G., Gantt, B., Foley, K., Fahey, K., Spero, T., Kang, D., Mathur, R., Foroutan, H., Xing, J., Sherwen, T., and Alfonso, S.-L.: Influence of bromine and iodine chemistry on annual, seasonal, diurnal, and background ozone: CMAQ simulations over the Northern Hemisphere, *Atmospheric Environment*, 213, <https://doi.org/10.1016/j.atmosenv.2019.06.020>, 2019.
- Sarwar, G., Hogrefe, C., Henderson, B. H., Mathur, R., Gilliam, R., Callaghan, A. B., Lee, J., and Carpenter, L. J.: Impact of particulate nitrate photolysis on air quality over the Northern Hemisphere, *Science of The Total Environment*, 917, 170406, <https://doi.org/https://doi.org/10.1016/j.scitotenv.2024.170406>, 2024.
- 410 Skamarock, W. C., Klemp, J. B., Dudhia, J., Gill, D. O., Barker, D. M., Duda, M. G., Huang, X.-Y., Wang, W., , and Powers, J. G.: A description of the Advanced Research WRF version 3, National Center for Atmospheric Research Tech. Note, NCAR/TN-475+STR, 113, 2008.
- 415 Skamarock, W. C., Klemp, J. B., Duda, M. G., Fowler, L. D., Park, S.-H., and Ringler, T. D.: A Multiscale Nonhydrostatic Atmospheric Model Using Centroidal Voronoi Tessellations and C-Grid Staggering, *Monthly Weather Review*, 140, 3090–3105, <https://doi.org/https://doi.org/10.1175/MWR-D-11-00215.1>, 2012.
- Wang, J., Wang, S., Jiang, J., Ding, A., Zheng, M., Zhao, B., Wong, D. C., Zhou, W., Zheng, G., Wang, L., Pleim, J. E., , and Hao, J.: Impact of aerosol-meteorology interactions on fine particle pollution during China’s severe haze episode in January 2013, *Environ. Res. Lett.*, 9, 2014.
- 420 Wiedinmyer, C., Akagi, S. K., Yokelson, R. J., Emmons, L. K., Al-Saadi, J. A., Orlando, J. J., and Soja, A. J.: The Fire INventory from NCAR (FINN): a high resolution global model to estimate the emissions from open burning, *Geoscientific Model Development*, 4, 625–641, <https://doi.org/10.5194/gmd-4-625-2011>, 2011.

- 425 Wong, D. C., Pleim, J., Mathur, R., Binkowski, F., Otte, T., Gilliam, R., Pouliot, G., Xiu, A., , and Kang, D.: WRF-CMAQ two-way coupled system with aerosol feedback: software development and preliminary results, *Geosci. Model Dev.*, 5, 299–312, 2012.
- Wong, D. C., Yang, C. E., Fu, J. S., Wong, K., and Gao, Y.: An approach to enhance pnetCDF performance in environmental modeling applications, *Geoscientific Model Development*, 8, 1033–1046, <https://doi.org/10.5194/gmd-8-1033-2015>, 2015.
- 430 Wong, D. C., Cai, C., Pleim, J., Mathur, R., , and Murphy, M. S.: Validation of the WRF-CMAQ Two-way Model with Aircraft Data and High Resolution MODIS Data in the CA 2008 Wildfire Case, 34th International Technical Meeting on Air Pollution Modeling and its Application, 2016.
- Xing, J., Mathur, R., Pleim, J., Hogrefe, C., Gan, C.-M., Wong, D. C., C., W., , and J., W.: Air pollution and climate response to aerosol direct radiative effects: a modeling study of decadal trends across the northern hemisphere, *Journal of Geophysical Research: Atmospheres*, 120, 12 221–12 236, 2015.
- 435 Xing, J., Mathur, R., Pleim, J., Hogrefe, C., Wang, J., Gan, C.-M., Sarwar, G., Wong, D. C., and McKeen, S.: Representing the effects of stratosphere–troposphere exchange on 3-D O<sub>3</sub> distributions in chemistry transport models using a potential vorticity-based parameterization, *Atmospheric Chemistry and Physics*, 16, 10 865–10 877, <https://doi.org/10.5194/acp-16-10865-2016>, 2016.
- Xiu, A. and Pleim, J. E.: Development of a land surface model. Part I: Application in a mesoscale meteorological model, *J. Appl. Meteor.*, 40, 192–209, 2001.
- 440 Zhao, B., Zheng, H., Wang, S., Smith, K., Lu, X., Aunan, K., Gu, Y., Wang, Y., Ding, D., Xing, J., Fu, X., Yang, X., Liou, K.-N., and Hao, J.: Change in household fuels dominates the decrease in PM<sub>2.5</sub> exposure and premature mortality in China in 2005–2015, *Proceedings of the National Academy of Sciences*, 115, 12 401–12 406, <https://doi.org/https://doi.org/10.1073/pnas.1812955115>, 2018.